Editors' Suggestion

Detailed Balance of Thermalization Dynamics in Rydberg-Atom Quantum Simulators

Hyosub Kim, YeJe Park, Kyungtae Kim, H.-S. Sim,* and Jaewook Ahn†
Department of Physics, KAIST, Daejeon 34141, Korea

(Received 13 February 2018; published 4 May 2018)

Dynamics of large complex systems, such as relaxation towards equilibrium in classical statistical mechanics, often obeys a master equation that captures essential information from the complexities. Here, we find that thermalization of an isolated many-body quantum state can be described by a master equation. We observe sudden quench dynamics of quantum Ising-like models implemented in our quantum simulator, defect-free single-atom tweezers in conjunction with Rydberg-atom interaction. Saturation of their local observables, a thermalization signature, obeys a master equation experimentally constructed by monitoring the occupation probabilities of prequench states and imposing the principle of the detailed balance. Our experiment agrees with theories and demonstrates the detailed balance in a thermalization dynamics that does not require coupling to baths or postulated randomness.

DOI: 10.1103/PhysRevLett.120.180502

It is a long-standing question about thermalization, whether and how an isolated many-body quantum system coherently evolves into a steady state that seems to be in thermal equilibrium [1,2]. As a variety of quantum simulators have been developed recently [3], there are a number of experimental reports on thermalization [4–7]. There are also theoretical mechanisms, such as the eigenstate thermalization hypothesis (ETH) [8–13], that tell us whether the steady state is practically indistinguishable from an equilibrium thermodynamic ensemble. By contrast, the principles of dynamics toward the steady state remain largely unknown. The thermalization dynamics has the complexity exponentially increasing with system size; hence, its computation is impractical for large systems. Recently, a master equation was derived [14] for describing the thermalization dynamics of a quantum spin system. It is constructed in terms of transition rates between the eigenstates of the prequench Hamiltonian and well describes the time evolution of local observables towards steady-state values (except some coherent oscillations). It is powerful, as the number of the rates necessary for the construction increases only linearly with system size. We experimentally construct the master equation by preparing optical dipole traps with unit occupation of ^{87}Rb atoms and monitoring the global sudden quench dynamics to a Rydberg level.

Rydberg-atom experiment.—We utilized the recently developed single-atom array synthesizer [15–18] in conjunction with global Rydberg-atom excitation. In Fig. 1(a), defect-free ^{87}Rb single-atom chains of various size ($N = 10$–25) were formed by using dynamic holographic optical tweezers; note the images of an $N = 25$ zigzag chain of bending angle $\theta = 60°$ in Fig. 1(b). We fixed the interatom distance $d = 4.0 \pm 0.2$ μm and changed the zigzag angle θ from 45° to 180°; among the angles θ's that we choose (see Supplemental Material in Ref. [19]), we focus on $\theta = 180°$ and 60°, which correspond to a spin chain with a nearest neighbor interaction and another with both of a nearest neighbor interaction and a next nearest neighbor interaction, respectively. The entire array was coherently driven to a $67S_{1/2}$ Rydberg state with homogeneous interaction strength by adopting widely used two-photon excitation [19,28–33]. Each atom i behaved as a pseudospin-1/2 system composed of the ground state $|5S_{1/2}, F = 2, m_F = 2\rangle \equiv |\downarrow_i\rangle$ and the Rydberg state $|67S_{1/2}, J = 1/2, m_J = 1/2\rangle \equiv |\uparrow_i\rangle$, as the intrinsic dephasing time 16 μs was longer than the experiment duration 3 μs [19].

The system can be described by the Hamiltonian of an Ising-like spin-1/2 chain [30–33],

$$H = H_0 + H_I = \sum_{i>j} V_{ij}\hat{n}_i\hat{n}_j + \sum_i \frac{\hbar\Omega}{2}\hat{\sigma}_x^{(i)} - \frac{\hbar\Delta}{2}\hat{\sigma}_z^{(i)}, \qquad (1)$$

where $\hat{n}_i = |\uparrow_i\rangle\langle\uparrow_i|$, $\hat{\sigma}_x^{(i)} = |\uparrow_i\rangle\langle\downarrow_i| + |\downarrow_i\rangle\langle\uparrow_i|$, and $\hat{\sigma}_z^{(i)} = |\uparrow_i\rangle\langle\uparrow_i| - |\downarrow_i\rangle\langle\downarrow_i|$. The first term H_0 of Eq. (1), the repulsive van der Waals interaction $V_{ij} = -C_6/|x_i - x_j|^6$ with coefficient $C_6 = -470$ GHz/μm^6 [34], behaves as interactions between the spins, while the second and third terms with Rabi frequency Ω and detuning Δ act as spin transverse Zeeman splitting H_I. The nearest neighbor interaction strength is estimated as $V_{12}/2\pi\hbar =$ 14–25 MHz for $d = 4.0 \pm 0.2$ μm, and the next nearest neighbor interaction strength V_{13} depends on θ, $V_{13} = V_{12}/64$ for $\theta = 180°$ and $V_{13} = V_{12}$ for $\theta = 60°$. The fluctuation of V_{ij} is due to thermal atomic motions. There is a shot-to-shot noise on H_I, resulting in 2 μs inhomogeneous dephasing time on collective Rabi oscillations [19]; however, it does not qualitatively alter the

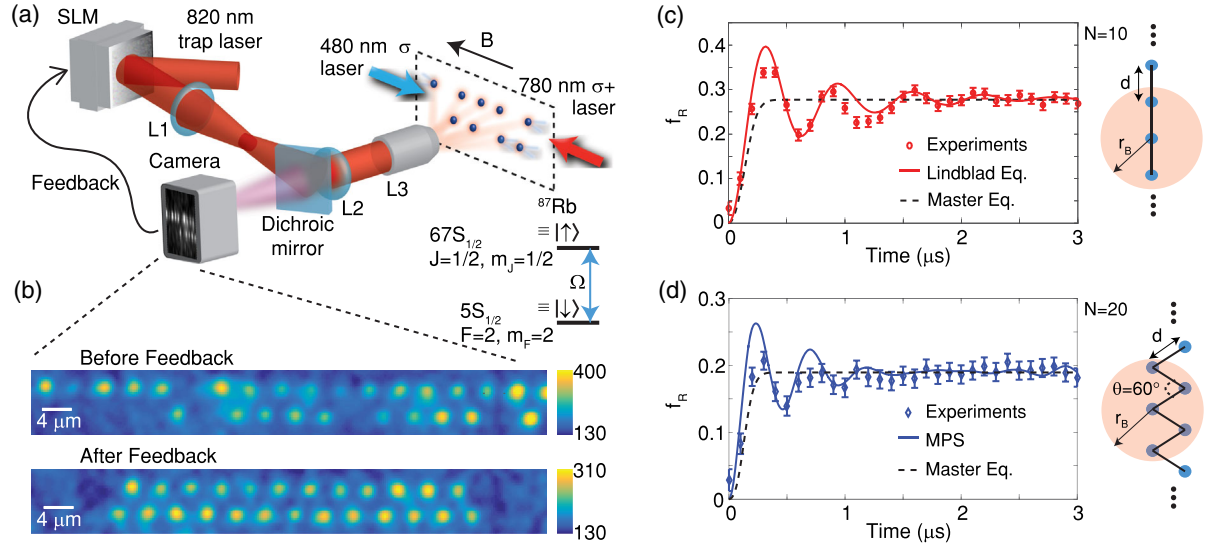

FIG. 1. Setup. (a) The wave front of the trap laser is modulated by a liquid-crystal spatial light modulator (SLM) and imaged by a telescope (L1, L2) and an objective lens (L3). The fluorescence image of the trapped atoms is captured by a camera and analyzed to feedback the SLM for array compactification by atom shuttling [15–18]. Then, 480 and 780 nm lasers excite the array to a $67S$ Rydberg state, forming a tunable Ising-like spin-1/2 chain. (b) Zigzag chain fluorescence images (Gaussian filtered for clarity). Time dependence of Rydberg fraction after the quench for (c) the linear chain of $N = 10$ and $\theta = 180°$ and (d) the zigzag chain of $N = 20$ and $\theta = 60°$. The experimental data (circles) are compared with the computation (solid lines) and the result (dashed) of the master equation constructed based on the experimental data. All error bars, ± standard error of the mean. (c),(d)(right) Chain configurations with blockade radius of $r_B = (|C_6|/2\pi\Omega)^{1/6} = 6.5$ μm and lattice spacing of $d = 4.0 \pm 0.2$ μm.

equilibration dynamics under the parameters of $H_0 \gg \hbar\Omega \gg \hbar|\Delta|$ [35].

Thermalization.—Initially, Ω and Δ are zero and the chain is in the ground state $|\downarrow_1\downarrow_2\ldots\downarrow_N\rangle$ of H_0. Then, staying at $t = 0$, they are suddenly turned onto $\Omega/2\pi = 1.0 \pm 0.1$ and $\Delta/2\pi = 0.0 \pm 0.1$ MHz. This global quench makes the measured Rydberg fraction $f_R \equiv \sum_i \langle\hat{n}_i\rangle(t)/N$ change in time, as in Figs. 1(c) and 1(d) [also see $\sum_{i,j}\langle\hat{n}_i\hat{n}_j\rangle(t)/N^2$ in Ref. [19]]. The overall features of f_R are qualitatively the same for $N \geq 10$; f_R shows coherent oscillations before it approaches a steady-state value $\bar{f}_R$. The major frequency component of the oscillations occurs at $\sqrt{2}\Omega$ for the linear chain and $\sqrt{3}\Omega$ for the zigzag chain of $\theta = 60°$, corresponding to the collective Rabi frequency of two or three atoms. The results agree with computations based on a Lindblad equation for $N = 10$ and on matrix product states (MPS, see Ref. [19]) for $N = 20$. Note that the shot-to-shot noise is taken into account for $N = 10$; the noise effect becomes negligible for larger N [5,11,36].

We estimate the relaxation time t_{relax}, after which the oscillations are suppressed, as $t_{\text{relax}} = 1.5$–2 μs from both of the experimental data and the theoretical calculation shown in Fig. 1; after the relaxation, there is still a long-time weak oscillation, which is a finite-size effect and becomes suppressed for larger N [5,11,36]. For smaller θ, t_{relax} becomes shorter (because of stronger next nearest neighbor interactions) and below the dephasing time (e.g., $t_{\text{relax}} = 1.5$ μs at $\theta = 60°$), implying that the relaxation may occur due more to the coherent dynamics than to the dephasing (experimental imperfection). For $N = 10$ and $\theta = 180°$, the inhomogeneous dephasing affects the relaxation, as the relaxation time $t_{\text{relax}} = 2$ μs becomes comparable to the dephasing time.

Around the relaxation time $t_{\text{relax}} = 1.5$–2 μs for $\theta = 60°$–$180°$, the oscillations are suppressed. We obtain the time average $\bar{f}_R$ at $t \geq t_{\text{relax}}$. $\bar{f}_R$ follows the universal scaling behavior of $\bar{f}_R \propto \alpha^{\nu}$ with $\alpha \propto \hbar\Omega d^6/|C_6|$ [19]. The measured exponent $\nu = 0.16 \pm 0.02$ agrees with the prediction [28,37] based on the Hamiltonian H. All the above observations support that our system properly works as Rydberg quantum simulators [31–33,38,39].

Detailed balance.—To analyze the relaxation of f_R, we measure the probabilities $P_n(t)$ with which there are n atoms in spin-up $|\uparrow\rangle$ at time t. In Fig. 2(a), $P_n(t)$ exhibits coherent oscillations while diffusing to a steady-state distribution. To describe the diffusion, we consider a master equation of the simplest form [14]

$$\partial_t P_n(t) = [P_{n+1}(t)\Gamma_{n+1\to n}(t) + P_{n-1}(t)\Gamma_{n-1\to n}(t)] - P_n(t)[\Gamma_{n\to n-1}(t) + \Gamma_{n\to n+1}(t)], \quad (2)$$

where $\Gamma_{n\to n\pm1}(t)$ is the rate of transition from states with n spin-up atoms to those with $n \pm 1$. The other transitions of $n \leftrightarrow n'(\neq n \pm 1)$ are negligible in our regime of $H_0 \gg H_I$,

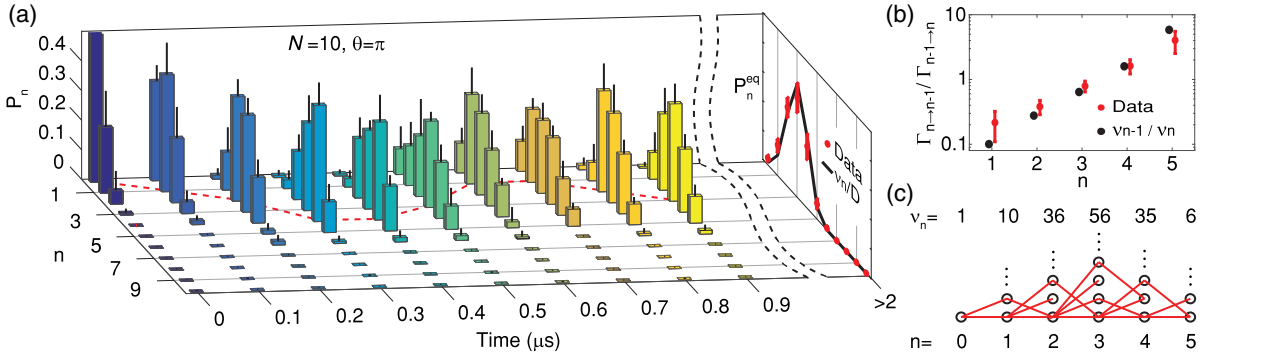

FIG. 2. Detailed balance in the linear chain of $N = 10$. (a) The measured $P_n(t)$ (color bars) and its standard deviation ($\pm\sigma$, overlaid black lines). At $t > 2\ \mu$s, the measured data (red dots) and the theoretical predictions (black line) of the steady-state values $P_n^{\rm eq}$ are shown. The red dashed line evolves along the tallest bar, showing the coherent oscillation of P_n. (b) The ratio $\Gamma_{n\to n-1}/\Gamma_{n-1\to n}$ (red dots) of transition rates are obtained (with error bar $\pm\sigma$) from $P_n^{\rm eq}$ and compared with the theoretical prediction (black dots). (c) Graph for the thermalization dynamics. Its nodes (circles) represent low-energy eigenstates of the prequench Hamiltonian H_0, classified by the number n of spin-up atoms in the states. ν_n is the number of the eigenstates having n spin-up atoms. Each red link connecting two nodes indicates transitions between the corresponding states by H_I.

as they are higher-order processes of multiple spin flips by H_I.

The principle of the detailed balance, $[P_{n+1}^{\rm eq}\Gamma_{n+1\to n} + P_{n-1}^{\rm eq}\Gamma_{n-1\to n}] = P_n^{\rm eq}[\Gamma_{n\to n-1} + \Gamma_{n\to n+1}]$ and $P_1^{\rm eq}\Gamma_{1\to 0} = P_0^{\rm eq}\Gamma_{0\to 1}$, is obtained from the master equation in the steady state, where $P_n = P_n^{\rm eq}$ and $\partial_t P_n(t) = 0$; equivalently, $\Gamma_{n\to n-1}/\Gamma_{n-1\to n} = P_{n-1}^{\rm eq}/P_n^{\rm eq}$. We obtain $P_n^{\rm eq}$ by the time average of $P_n(t)$ at $t \geq t_{\rm relax}$ and retrieve the microscopic information of $\Gamma_{n\to n-1}/\Gamma_{n-1\to n}$ using the detailed balance relation. In Fig. 2, the results agree with the theoretical prediction [14,40] of $P_n^{\rm eq} = \nu_n/D$ and $\Gamma_{n\to n-1}/\Gamma_{n-1\to n} = \nu_{n-1}/\nu_n$ obtained in the limit of $H_I/H_0 \to 0$, where $\nu_n = \binom{N+1-n}{n}$ for the linear chain, $\nu_n = \binom{N+2-2n}{n}$ for $\theta = 60°$, and $D = \sum_n \nu_n$.

We explain the meaning of ν_n for the linear chains as an example. In our relaxation dynamics, $H_0 \gg H_I$ and the initial state is the ground state $|\downarrow_1\downarrow_2\cdots\downarrow_N\rangle$ of H_0. In this case, it is enough to consider only low-energy eigenstates $|\sigma_z^{(1)}\sigma_z^{(2)}\ldots\sigma_z^{(N)}\rangle$ of the prequench Hamiltonian H_0, from $|\downarrow_1\downarrow_2\downarrow_3\ldots\rangle$ to $|\uparrow_1\downarrow_2\uparrow_3\ldots\rangle$, in which any two neighboring spins $\sigma_z^{(i)}$ and $\sigma_z^{(i+1)}$ cannot be simultaneously in spin-up; the other higher-energy eigenstates can be ignored, since they are separated from the low-energy states in energy at least by $V_{i,i+1}$. Then, $P_n(t)$ almost equals the probability of occupying the low-energy states of n spin-up atoms, and the possible values of n are $0, 1, \ldots, n_{\rm max} = N/2$ for even N and $0, 1, \ldots, n_{\rm max} = (N+1)/2$ for odd N. ν_n is the number of the low-energy states of n spin-up atoms. Transitions between those of n and those of $n \pm 1$, occurring with a single spin flip by H_I, govern the relaxation dynamics in our regime of $H_0 \gg H_I$ [14]. In this case, the ratio $\Gamma_{n\to n-1}/\Gamma_{n-1\to n}$ of the transition rates equals the ratio ν_{n-1}/ν_n. We emphasize that the ratios, microscopic information of the dynamics, are measured in our experiments.

The master equation in Eq. (2) efficiently describes the relaxation dynamics, as it has only $2n_{\rm max}$ parameters of the transition rates $\Gamma_{n\to n\pm 1}$, which is much smaller than the size 2^N of the Hilbert space. This allows us to experimentally construct the master equation. Among the $2n_{\rm max}$ parameters, $n_{\rm max}$ parameters are determined by the ratios $\Gamma_{n\to n-1}/\Gamma_{n-1\to n}$, measured by applying the detailed balance. The other $n_{\rm max}$ parameters are determined by using the probabilities $P_n(t)$ and their derivatives $\partial_t P_n(t)$ measured at the early stage of $t \simeq 0$ before the coherent oscillations occur. In this step, we use the form of $\Gamma_{n\to n\pm 1}(t) = 2\Omega^2 t T_{n\to n\pm 1}$ derived in Ref. [14], where $T_{n\to n\pm 1}$'s are time independent. Using the experimentally constructed master equation, we compute the time evolution of the Rydberg fraction $f_R(t)$ [$= \sum_n n P_n(t)/N$] and $\sum_{i,j}\langle\hat{n}_i\hat{n}_j\rangle(t)/N^2$ [$= \sum_n n^2 P_n(t)/N^2$] and find that the result well describes the experimental data of the relaxation of $f_R(t)$ in Figs. 1(c) and 1(d) [Ref. [19] for $\sum_{i,j}\langle\hat{n}_i\hat{n}_j\rangle(t)/N^2$]. Note that the master equation result does not show the coherent oscillations, since the higher-energy eigenstates and the processes of multiple spin flips are ignored in the master equation. All the observations imply that the thermalization dynamics obeys the master equation, similar to dynamics to equilibrium in statistical mechanics.

Steady state.—The thermalization dynamics can be considered as diffusion on the graph in Fig. 2(c), where each link has equal transition probability determined by H_I. This indicates that the relaxation time $t_{\rm relax}$ depends on the initial point of the diffusion [14,40]. The initial state $|\downarrow_1\downarrow_2\ldots\downarrow_N\rangle$ of this experiment is located at an edge of the graph. Hence, the dynamics has a long relaxation time $t_{\rm relax}$ as in Figs. 1(c), 1(d), and 2(a). When an initial state is located closer to the center of the graph, the resulting coherent oscillations become more rapidly suppressed with shorter $t_{\rm relax}$ [14].

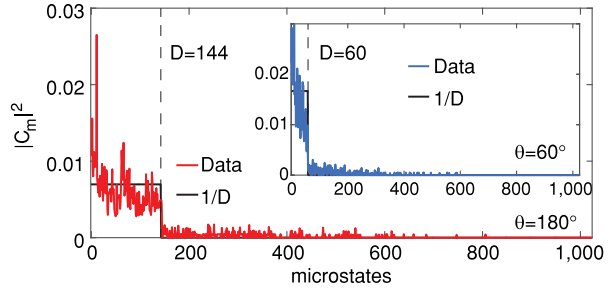

FIG. 3. Diffusion over prequench states. Time average ($t \geq t_{\mathrm{relax}}$) of the measured probability $|C_m|^2$ of occupying the mth eigenstates of the prequench Hamiltonian H_0 for the linear chain of $N = 10$. The position of the Dth eigenstate is indicated by the dashed line. (Inset) The same for the $\theta = 60°$ zigzag chain of $N = 10$.

We experimentally measured the steady-state values of the probability $|C_m|^2$ with which the chain occupied the mth eigenstate of the prequench Hamiltonian H_0. In the language of the diffusion on the graph, $|C_m|^2$ is interpreted as the occupation probability of the node corresponding to the mth eigenstate. As shown in Fig. 3, the result is $|C_m|^2 \simeq 1/D$, where $D = \sum_n \nu_n$ is the total number of the low-energy eigenstates. This demonstrates almost uniform spreading over the graph, namely, over the low-energy eigenstates. Indeed, the experimental data of P_n^{eq} are close to ν_n/D.

In Fig. 4, the experimental results of the steady-state values of the Rydberg fraction f_R are shown for $N = 3$–25. They agree with the computation based on the MPS. They are, however, slightly different from the ETH prediction.

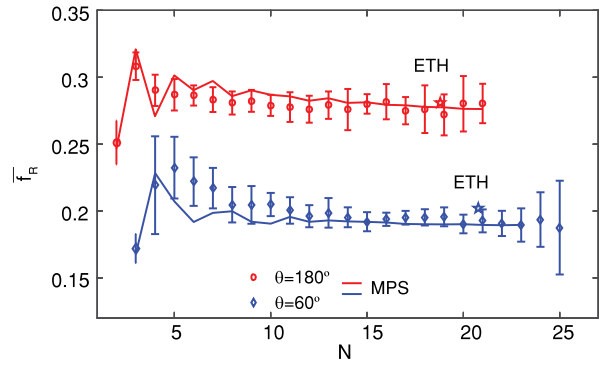

FIG. 4. Thermalization value. Time average $\bar{f}_R$ of the measured Rydberg fraction as a function of system size N for the linear chain (red circles) and the zigzag chain of $\theta = 60°$ (blue diamonds). The error bars of $\pm\sigma$ are shown. For comparison, the MPS result (solid lines) and the ETH prediction (at $N = 19$ for the linear chain and at $N = 21$ for the zigzag chain; color stars) are shown. Note that the data points of the shortest chains ($N = 2$, $\theta = 180°$) and ($N = 3$, $\theta = 60°$) have smaller error bars than the other points, because they are obtained from a data set for which a defect-free chain is formed from a chain of smaller initial size.

Indeed, the typical features of the ETH do not hold in our cases [19].

In summary, we performed a quantum simulation experiment with tunable tweezer traps and Rydberg-atom interaction. Our quantum simulator provides an ideal test bed for studying quantum coherent evolution of a many-body system after a quench. It allows us to simulate a one- or two-dimensional lattice of Ising-like spin-1/2 particles or the Hamiltonian in Eq. (1) with parameters tunable in a wide range. We can monitor the time evolution by measuring occupation probabilities of the eigenstates of a prequench Hamiltonian or a postquench Hamiltonian. The thermalization dynamics studied in our experiment belongs to the cases where the postquench Hamiltonian is slightly modified after quench so that $H_0 \gg H_I$. Our results suggest that the detailed balance can be an underlying principle of the thermalization dynamics of the cases. The thermalization dynamics can be efficiently described by the diffusion governed by a master equation of a simple form, similar to relaxation towards equilibrium in classical statistical mechanics, but without its underlying assumptions of coupling to baths and the ergodicity hypothesis based on randomness.

We acknowledge technical support from Woojun Lee and Minhyuk Kim and fruitful discussions with Yunheung Song and Dr. Chae-Yeun Park. This research was supported by the Samsung Science and Technology Foundation [SSTF-BA1301-12] and Korea National Research Foundation [2016R1A5A1008184].

*hssim@kaist.ac.kr
†jwahn@kaist.ac.kr

[1] A. Polkovnikov, K. Sengupta, A. Silva, and M. Vengalattore, Rev. Mod. Phys. **83**, 863 (2011).
[2] G. Christian and E. Jens, Rep. Prog. Phys. **79**, 056001 (2016).
[3] H. Weimer, M. Muller, I. Lesanovsky, P. Zoller, and H. P. Buchler, Nat. Phys. **6**, 382 (2010).
[4] T. Langen, R. Geiger, M. Kuhnert, B. Rauer, and J. Schmiedmayer, Nat. Phys. **9**, 640 (2013).
[5] G. Clos, D. Porras, U. Warring, and T. Schaetz, Phys. Rev. Lett. **117**, 170401 (2016).
[6] A. M. Kaufman, M. E. Tai, A. Lukin, M. Rispoli, R. Schittko, P. M. Preiss, and M. Greiner, Science **353**, 794 (2016).
[7] C. Neill, P. Roushan, M. Fang, Y. Chen, M. Kolodrubetz, Z. Chen, A. Megrant, R. Barends, B. Campbell, B. Chiaro *et al.*, Nat. Phys. **12**, 1037 (2016).
[8] J. M. Deutsch, Phys. Rev. A **43**, 2046 (1991).
[9] M. Srednicki, Phys. Rev. E **50**, 888 (1994).
[10] M. Srednicki, J. Phys. A **32**, 1163 (1999).
[11] M. Rigol, V. Dunjko, and M. Olshanii, Nature (London) **452**, 854 (2008).
[12] M. Rigol and M. Srednicki, Phys. Rev. Lett. **108**, 110601 (2012).

[13] L. D'Alessio, Y. Kafri, A. Polkovnikov, and M. Rigol, Adv. Phys. **65**, 239 (2016).
[14] C. Ates, J. P. Garrahan, and I. Lesanovsky, Phys. Rev. Lett. **108**, 110603 (2012).
[15] H. Kim, W. Lee, H.-g. Lee, H. Jo, Y. Song, and J. Ahn, Nat. Commun. **7**, 13317 (2016).
[16] W. Lee, H. Kim, and J. Ahn, Phys. Rev. A **95**, 053424 (2017).
[17] D. Barredo, S. de Léséleuc, V. Lienhard, T. Lahaye, and A. Browaeys, Science **354**, 1021 (2016).
[18] M. Endres, H. Bernien, A. Keesling, H. Levine, E. R. Anschuetz, A. Krajenbrink, C. Senko, V. Vuletic, M. Greiner, and M. D. Lukin, Science **354**, 1024 (2016).
[19] See Supplemental Material at http://link.aps.org/supplemental/10.1103/PhysRevLett.120.180502, which includes Refs. [20–27].
[20] K. M. Maller, M. T. Lichtman, T. Xia, Y. Sun, M. J. Piotrowicz, A. W. Carr, L. Isenhower, and M. Saffman, Phys. Rev. A **92**, 022336 (2015).
[21] X. L. Zhang, A. T. Gill, L. Isenhower, T. G. Walker, and M. Saffman, Phys. Rev. A **85**, 042310 (2012).
[22] Y. Miroshnychenko, A. Gaëtan, C. Evellin, P. Grangier, D. Comparat, P. Pillet, T. Wilk, and A. Browaeys, Phys. Rev. A **82**, 013405 (2010).
[23] I. I. Beterov, I. I. Ryabtsev, D. B. Tretyakov, and V. M. Entin, Phys. Rev. A **79** 052504 (2009).
[24] U. Schollwöck, Rev. Mod. Phys. **77**, 259 (2005).
[25] B. Pirvu, V. Murg, J. I. Cirac, and F. Verstraete, New J. Phys. **12**, 025012 (2010).
[26] F. Verstraete, J. J. García-Ripoll, and J. I. Cirac, Phys. Rev. Lett. **93**, 207204 (2004).
[27] F. Verstraete, V. Murg, and J. I. Cirac, Adv. Phys. **57**, 143 (2008).
[28] R. Low, H. Weimer, J. Nipper, J. B. Balewski, B. Butscher, H. P. Buchler, and T. Pfau, J. Phys. B **45**, 113001 (2012).
[29] J. Zeiher, P. Schauß, S. Hild, T. Macrí, I. Bloch, and C. Gross, Phys. Rev. X **5**, 031015 (2015).
[30] P. Schauß, J. Zeiher, T. Fukuhara, S. Hild, M. Cheneau, T. Macrí, T. Pohl, I. Bloch, and C. Gross, Science **347**, 1455 (2015).
[31] H. Labuhn, D. Barredo, S. Ravets, S. de Léséleuc, T. Macrí, T. Lahaye, and A. Browaeys, Nature (London) **534**, 667 (2016).
[32] H. Bernien, S. Schwartz, A. Keesling, H. Levine, A. Omran, H. Pichler, S. Choi, A. S. Zibrov, M. Endres, M. Greiner *et al.*, Nature (London) **551**, 579 (2017).
[33] V. Lienhard, S. de Léséleuc, D. Barredo, T. Lahaye, A. Browaeys, M. Schuler, L.-P. Henry, and A. M. Lauchli, arXiv:1711.01185.
[34] W. Sebastian, T. Christoph, M. Henri, U. Alban, F. Ofer, B. Hans Peter, and H. Sebastian, J. Phys. B **50**, 133001 (2017).
[35] I. Lesanovsky, B. Olmos, and J. P. Garrahan, Phys. Rev. Lett. **105**, 100603 (2010).
[36] T. Kiendl and F. Marquardt, Phys. Rev. Lett. **118**, 130601 (2017).
[37] H. Weimer, R. Löw, T. Pfau, and H. P. Büchler, Phys. Rev. Lett. **101**, 250601 (2008).
[38] M. Marcuzzi, J. Minár, D. Barredo, S. de Léséleuc, H. Labuhn, T. Lahaye, A. Browaeys, E. Levi, and I. Lesanovsky, Phys. Rev. Lett. **118**, 063606 (2017).
[39] E. Guardado-Sanchez, P. T. Brown, D. Mitra, T. Devakul, D. A. Huse, P. Schauß, and W. S. Bakr, arXiv:1711:00887.
[40] B. Olmos, M. Muller, and I. Lesanovsky, New J. Phys. **12**, 013024 (2010).